University of Groningen

Cationic Gold(I) Diarylallenylidene Complexes

Sorbelli, Diego; Comprido, Laura Nunes dos Santos; Knizia, Gerald; Hashmi, A. Stephen K.; Belpassi, Leonardo; Belanzoni, Paola; Klein, Johannes E. M. N.

IMPORTANT NOTE: You are advised to consult the publisher's version (publisher's PDF) if you wish to cite from it. Please check the document version below.

Document Version
Publisher's PDF, also known as Version of record

Link to publication in University of Groningen/UMCG research database

Cationic Gold(I) Diarylallenylidene Complexes: Bonding Features and Ligand Effects

Diego Sorbelli,[a] Laura Nunes dos Santos Comprido,[b, c] Gerald Knizia,[d]
A. Stephen K. Hashmi,[c, e] Leonardo Belpassi,[f] Paola Belanzoni,*[a, f] and
Johannes E. M. N. Klein*[b]

Using computational approaches, we qualitatively and quantitatively assess the bonding components of a series of experimentally characterized Au(I) diarylallenylidene complexes (N.Kim, R.A.Widenhoefer, *Angew. Chem. Int. Ed.* **2018**, *57*, 4722–4726). Our results clearly demonstrate that Au(I) engages only weakly in π-backbonding, which is, however, a tunable bonding component. Computationally identified trends in bonding are clearly correlated with the substitution patterns of the aryl substituents in the Au(I) diarylallenylidene complexes and good agreement is found with the previously reported experimental data, such as IR spectra, ^{13}C NMR chemical shifts and rates of decomposition together with their corresponding barrier heights, further substantiating the computational findings. The description of the bonding patterns in these complexes allow predictions of their spectroscopic features, their reactivity and stability.

1. Introduction

Gold allenylidene complexes[1] are potentially interesting intermediates in the field of gold catalysis,[2] due to the presence of two reactive electrophilic carbon atoms. However, only a few examples of well-defined gold allenylidene complexes have been reported in the literature (Figure 1, top),[3] where such complexes usually rely on the stabilization through heteroatom substituents. Recently, Kim and Widenhoefer synthesized and characterized a series of gold(I) diarylallenylidene complexes with varying substituents on the aryl groups of which we show five examples (complexes **a**–**e** in Figure 1 (bottom).[4] These complexes are distinct, as they lack stabilizing heteroatoms.

Figure 1. Examples of Au allenylidene complexes featuring hetero atom substitution (top).[3] Reported Au(I) diarylallenylidene complexes (**a**–**e**)[4] considered in this work. Resonance structures describing the carbocation (**I**), allenylidene (**II**) and delocalized carbocation (**III**) forms of the complexes. In computations we consider a truncated version of the NHC ligand where the aryl substituents are replaced by Me groups.

[a] D. Sorbelli, Prof. Dr. P. Belanzoni
     Dipartimento di Chimica, Biologia e Biotecnologie
     Università degli Studi di Perugia
     Via Elce di Sotto 8, 06123 Perugia, Italy
     E-mail: paola.belanzoni@unipg.it
[b] Dr. L. Nunes dos Santos Comprido, Dr. J. E. M. N. Klein
     Molecular Inorganic Chemistry, Stratingh Institute for Chemistry
     Faculty of Science and Engineering, University of Groningen
     Nijenborgh 4, 9747 AG Groningen, The Netherlands
     E-mail: j.e.m.n.klein@rug.nl
[c] Dr. L. Nunes dos Santos Comprido, Prof. Dr. A. S. K. Hashmi
     Organisch-Chemisches Institut
     Ruprecht-Karls-Universität Heidelberg
     Im Neuenheimer Feld 270, 69120 Heidelberg, Germany
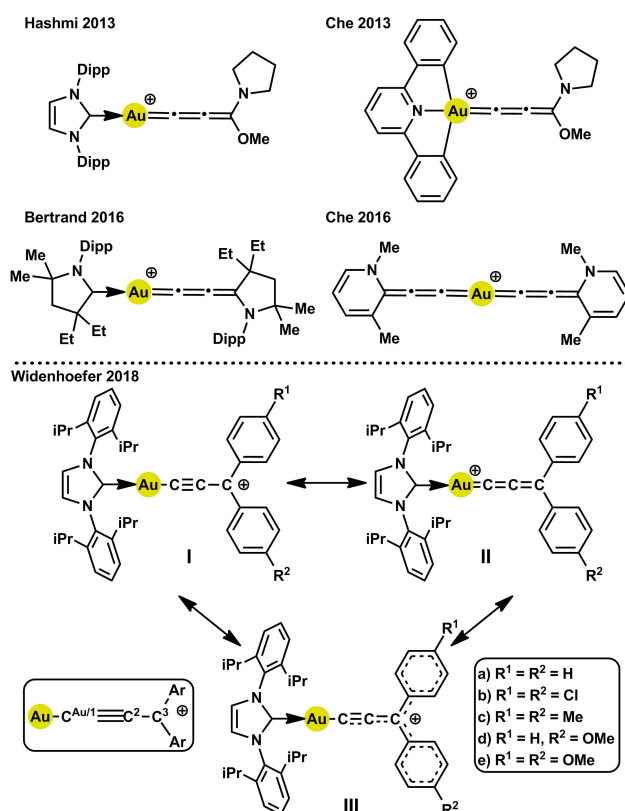[d] Prof. Dr. G. Knizia
     Department of Chemistry, Pennsylvania State University
     401A Chemistry Bldg; University Park, PA 16802, USA
[e] Prof. Dr. A. S. K. Hashmi
     Chemistry Department, Faculty of Science
     King Abdulaziz University, Jeddah 21589, Saudi Arabia
[f] Dr. L. Belpassi, Prof. Dr. P. Belanzoni
     Istituto di Scienze e Tecnologie Molecolari del CNR (CNR-ISTM)
     c/o Dipartimento di Chimica, Biologia e Biotecnologie
     Università degli Studi di Perugia, via Elce di Sotto 8, Perugia 06123, Italy

Supporting information for this article is available on the WWW under https://doi.org/10.1002/cphc.201900411

Examples of non-heteroatom stabilized complexes have been reported in the literature for gold carbenes, but they are also scarce (vide infra). In a recent review on complexes of group 10 and 11 metals with non-heteroatom stabilized carbene ligands, Peloso and Carmona[5] encourage chemists to concentrate further efforts on this new family of organometallic compounds in view of both their intrinsic structural value and their potential interest in catalysis. A breakthrough in this research area was the isolation and characterization of the first non-heteroatom substituted gold carbene, $[Cy_3PAuCAr_2]NTf_2$ (Ar=p-MeOC$_6$H$_4$), in the solid state by Seidel and Fürstner.[6] The authors found modest Au—C double bond character, consistent with a small backdonation from gold to the carbene center, and in agreement with computational studies of this complex.[7] The organic ligand framework is responsible for stabilizing this species by resonance delocalization of the accumulated positive charge. The first example of a gold carbene complex that lacks conjugated heteroatom stabilization of the carbene C atom was reported by Harris and Widenhoefer.[8] They synthesized and characterized a stable cycloheptatrienylidene complex, $[(P)$ $Au-\eta^1-C_7H_6)]BF_4$ (P=P(^{t}Bu)$_2$(o-biphenyl)), where, in the absence of heteroatoms, the involvement of the empty 2p orbital of the carbenic C atom in the aromatic π system of the tropylium cation was recognized to play a crucial role in stabilizing this species. A further contribution to this topic was made by Straub and co-workers who were able to isolate and characterize a non-heteroatom stabilized gold carbene complex, $[(IPr^{**})$ $Au=CMes_2]NTf_2$, with predominant carbenium character.[9] Work by Bourissou and co-workers proposed a novel approach for improving the stability of the carbene in gold cationic alkylidenes complexes on the basis of a suitable design of the ancillary ligand L to enhance the π backdonation ability of the $[LAu]^+$ moiety. This was achieved by employing the sterically demanding o-bis(aminophosphino)carborane, DPC, which is able to promote the electron density transfer to the empty 2p orbital of the carbenic C atom through the bending of the two-coordinate $(DPC)Au^+$ fragment.[10]

The related gold(I) diarylallenylidene complexes reported by Kim and Widenhoefer shown in Figure 1 (bottom) have been characterized by means of IR and NMR spectroscopy (and X-ray crystallography for complex e. In addition, rates of decomposition together with their corresponding barrier heights for this series of complexes have been determined, allowing for direct insight into the role of the substituents.

The results from this experimental study can be clearly interpreted: Going from complex a to e, the increasing electron-donor strength of the substituent causes a progressive blue shift of the C^1-C^2 stretching frequency. Similar trends are observed for ^{13}C NMR chemical shifts: both on the C^1 and C^3 atoms, where a progressive shielding is measured when the electron-donor ability of the substituent increases. The crystal structure of complex e shows that the anisyl groups are slightly twisted out of the plane and that C—C bonds between C^3 and the aromatic residues are relatively short (1.436 Å).[4] A well-defined trend is found for the rates of decomposition together with their corresponding barrier heights: Going from complex a to e, the stability increases, which is in accordance with the

expectation that such cationic species are electrophilic and benefit from the presence of electron donating substituents.

Based on these well-defined experimental trends, an investigation into the bonding features of these complexes should provide insight on how the substituents modulate stability and reactivity.

As depicted in Figure 1, one can formulate two mesomeric structures for the depiction of these complexes, where they are either depicted as an alkyne bound to gold featuring a carbocation (I), a true allenylidene (II) or a delocalized carbocation that benefits from stabilization through π-donation (III). One might therefore ask: What structure is the most suitable depiction of these complexes? For Au carbene complexes this seemingly simple question led to a debate in the past.[11] The focus was the nature of the Au—C bond, and whether these are best described as true gold carbene complexes, and hence have double bond character, or as gold-stabilized carbocations with a Au—C single bond. For the related allenylidene complexes, the mesomeric form (II) indicates σ-donor and π-acceptor interaction depicted as a Au—C double bond. In contrast to this depiction, (I) has a Au—C single bond and retains a C—C triple bond, much like in the precursors used in their synthesis. In the study of Kim and Widenhoefer the C^1-C^2 stretching frequencies for complex a and the corresponding Au-acetylide precursor are reported to only differ by 69 cm^{-1},[4] raising the question how much of the triple bond is preserved and how much double bond character is present in the Au—C interaction. In an additional Lewis structures depiction one can also envision a fully delocalized carbocation where the alkyne and both aromatic rings can function as a π-donor. One of the tools that has proven very helpful in this context is the Charge Displacement (CD) method,[12] that allows to disentangle and quantify the Dewar-Chatt-Duncanson (DCD)[13] components of the coordination bond, through analysis of the σ-donation and π-backdonation. In addition, some of us pointed out in previous studies[7,14] that the substituents on carbene complexes are of significant importance as these result in stabilization through π-donation as uncovered by the use of the intrinsic bond orbital (IBO)[15] method.

In the present study we apply both of these approaches to clarify the bonding in Au(I) allenylidene complexes and what the most suitable Lewis structure depiction is.

Experimental Section

CD-NOCV Method

The Charge Displacement (CD)[12a,b] method provides a clear and unequivocal description of the DCD[13] components of a bond between two fragments forming an adduct. The CD function is described as partial progressive integration on a suitable z axis of the electron density difference $\Delta\rho(x, y, z')$ between the density of the adduct and the sum of the densities of the non-interacting separated fragments at the positions they have in the adduct geometry [Eq. (1)]:[12a]

$$\Delta q(z) = \int_{-\infty}^{+\infty} dx \int_{-\infty}^{+\infty} dy \int_{-\infty}^{z} \Delta\rho(x,y,z') dz' \qquad (1)$$

In our calculations the two fragments are the metal fragment (i.e. Au bonded to the carbene ligand) and the diarylallenylidene ligand and therefore the z axis is the bond axis between these two fragments.

The CD function, at each z point, evaluates the amount of electrons flowing along the z direction. To quantify it, a plane along the z axis must be chosen and conventionally the charge flow is measured at the "isodensity boundary",[12b] which is the point where the densities of the two non-interacting fragments become equal. Following this convention, we quantify here the amount of electrons passing through the plane at the isodensity boundary which is defined as Charge Transfer or CT: positive CT values identify charge flowing from the right to the left, whereas negative CT values identify charge flowing from the left to the right.

In order to disentangle the DCD components of the bond, $\Delta\rho(x, y, z')$ must be partitioned into contributions. Usually, this can be done for symmetric systems according to the irreducible representations of the symmetry point group. Since the complexes under study have no symmetry, a method for a $\Delta\rho$ decomposition in non-symmetric systems within the Natural Orbitals for Chemical Valence (NOCVs)[12c,16] framework is used.

In the CD-NOCV framework, the charge rearrangement taking place upon the bond formation is obtained from the occupied orbitals of the two fragments suitably orthogonalized to each other and renormalized ("promolecule"). The resulting electron charge density rearrangement $\Delta\rho'$ can be written in terms of NOCV pairs, i.e. the eigenfunctions $\phi_{\pm k}$ of the so-called "valence operator" of Nalewajski and Mrozek valence theory,[17] as follows [Eq. (2)]:

$$\Delta\rho' = \sum_{k} \Delta\rho'_k \qquad (2)$$

where k is the index that pairs the NOCVs.

However, only a small subset of these NOCV pairs actually contributes to the overall charge rearrangement $\Delta\rho'$ because a large part of them presents eigenvalues close to zero.[18] The CD-NOCV approach has been successfully applied for the characterization of transition metal compounds[19] and for disentangling donation and backdonation in the CD function of non-symmetric systems containing NHC—Au(I) bond,[20] Au(I)—H bond[21] or Au(III)—CO bond with different ancillary ligands.[22]

Well-defined measurements of the total charge transfer (denoted as CT^{net}) and of its σ donation and perpendicular and parallel π backdonation contributions (denoted as CT$^{\sigma-don}$, CT$^{\pi-back}_{\perp}$ and CT$^{\pi-back\parallel}$, respectively) are obtained by evaluating the corresponding CD-NOCV function at the "isodensity boundary".

EDA Method

EDA (Energy Decomposition Analysis)[23] has been applied to obtain a more complete description of the bond. The EDA approach allows to decompose the interaction energy (ΔE_{int}) between two fragments constituting a molecule in three different terms [Eq. (3)]:

$$\Delta E_{int} = \Delta E_{elst} + \Delta E_{Pauli} + \Delta E_{oi} \qquad (3)$$

where ΔE_{elst} is the quasi-classical electrostatic interaction between the fragments, ΔE_{Pauli} (Pauli repulsion) is the repulsion between

occupied orbitals of the two fragments and ΔE_{oi} (orbital interaction) arises from the orbital relaxation and the orbital mixing between the fragments, accounting for electron pair bonding, charge transfer and polarization. The sum of ΔE_{elst} and ΔE_{Pauli} terms is conceived as the steric interaction, ΔE^0.

IAO Method[15]

Self-consistent field methods like Kohn-Sham DFT or Hartree-Fock allow quantitative predictions of many physical properties. Unfortunately, this requires expanding their occupied orbitals $\varphi_i(r)$ using large and flexible basis sets (e.g. triple zeta or larger), which have too large a variational freedom to allow for a unique assignment of basis functions to the individual atoms they are placed on. Intrinsic Atomic Orbitals (IAOs) are a method to restore an interpretable picture of the orbital expansion compatible with chemical intuition. IAOs constitute a minimal basis set of atomic core and valence orbitals (AOs), in which each IAO $\omega_\rho(r)$ can be uniquely assigned to a given atom-for example, a Carbon atom has only five IAOs (1 s, 2 s, 2p$_x$, 2p$_y$, 2p$_z$). However, unlike a regular minimal basis set, which is meant to represent AOs of *free* atoms, the IAOs are polarized as needed to represent the atomic orbitals in a given molecule. For this, the IAOs $\omega_\rho(r)$ are themselves expressed as a linear expansion over the basis functions $\chi_\mu(r)$ of the full computational basis set B_1 [Eq. (4)]:

$$\omega_\rho(r) = \sum_{\mu \in B_1} R_\rho^\mu \chi_\mu(r) \qquad (4)$$

The coefficients R_ρ^μ are determined in such a way that IAOs span exactly the occupied molecular orbitals $\varphi_i(r)$ of a given SCF wave function, but otherwise resemble the tabulated free-atom AOs as closely as possible (before orthogonalization of the IAOs). This yields IAOs $\omega_\rho(r)$ uniquely associated with the electronic degrees of freedom of each atom, unlike the normal basis functions $\chi_\mu(r)$, but still capable of exactly expressing the given occupied orbitals $\varphi_i(r)$.

IBO Method[15]

Since the IAOs $\omega_\rho(r)$ span the occupied molecular orbitals $\varphi_i(r)$, it is possible to re-express the latter as a linear combination over IAOs [Eq. (5)]:

$$\varphi_i(r) = \sum_{\rho \in B_2} \tilde{O}_i^\rho \omega_\rho(r) \qquad (5)$$

The advantage of this construction is that we now can unambiguously split each molecular orbital $\varphi_i(r)$ into its atomic contributions-we get a true linear combination of atomic orbitals (LCAO), rather than just a linear combination of basis functions. In particular, we can now uniquely define the electron occupation $n_A(i)$ of each orbital i on any atom A.

IBOs are obtained by combining this charge definition with the unitary invariance of Slater determinant wave functions create a physically equivalent local picture of the occupied orbitals. Concretely, if we replace a Slater determinant's occupied orbitals $\varphi_i(r)$ by a new set of occupied orbitals [Eq. (6)]:

$$\bar{\varphi}_i(r) = \sum_{j}^{occ} \varphi_j(r) U_{ji} \qquad (6)$$

in which the U_{ji} are the elements of a unitary matrix, then even if the individual sets of orbitals $\varphi_i(r)$ and $\bar{\varphi}_i(r)$ (one-particle wave

functions) look radically different, the actual N-electron wave function originating from either set-and this is the only physically relevant object-is physically equivalent. In the IBO method this freedom is used to compute a set of localized occupied molecular orbitals $\bar{\varphi}_i(\mathbf{r})$ in such a way that the orbital charge is spread over as few atoms as possible. Concretely, the unitary matrix U_{ji} is computed in such a way that for the new orbitals $\bar{\varphi}_i(\mathbf{r})$ the following localization functional becomes maximal, similar to the procedure reported by Pipek and Mezey [Eq. (7)]:[24]

$$L = \sum_j^{occ} \sum_A^{atoms} |n_A(i')|^2 \qquad (7)$$

Despite the fact that these definitions are purely mathematical and invoke few empirical chemical concepts, we have previously shown that the IBOs resulting from this construction very closely resemble what most chemists would understand "sigma bonds", "pi-bonds", and other types of lone-pair and bond orbitals to look like. However, the purely mathematical definition allows using IBOs to analyze new and unknown bonding situations, as well as to following their transformations across reaction paths.[25]

Computational Details

Calculations were carried out using model complexes where the two isopropylphenyl groups in IPr (1,3-bis-(2,6-diisopropylphenyl) imidazol-2-ylidene) were replaced by methyl groups (model NHC = 1,3-dimethylimidazol-2-ylidene). Geometry optimizations, frequency calculations, NOCV densities used in the CD analysis and Energy Decomposition Analysis, were performed using Density Functional Theory (DFT) as implemented in the Amsterdam Density Functional (ADF) package (2014.05 version).[26] The BP86 functional[27] was used in combination with the Slater-type TZ2P quality basis set[28] (with small frozen core) for all atoms and a scalar ZORA[29] Hamiltonian was used to account for relativistic effects.

For the IBO analysis,[15] single point energy calculations were carried out in TURBOMOLE v7.0.2[30] using the TPSS functional,[31] Grimme's D3 dispersion correction[32] with Becke-Johnson damping[32b] in combination with the def2-TZVPP basis set[33] and grid m5 was used. An effective core potential (ECP) was used for gold.[34] MARI-J (multipole accelerated resolution of identity approach)[35] was used to increase computational efficiency using Weigend's fitting basis set.[36]

2. Results and Discussion

We began our investigation by optimizing model complexes where two isopropylphenyl groups in IPr (1,3-bis-(2,6-diisopropylphenyl)imidazol-2-ylidene) were replaced with methyl groups (model NHC = 1,3-dimethylimidazol-2-ylidene) for **a-e** at the BP86/TZ2P/ZORA level of theory.[27–29] Based on these geometries we carried out the Charge Displacement (CD) analysis at the same level of theory. In addition, we computed Kohn-Sham wavefunctions at the TPSS-D3(BJ)/def2-TZVPP level of theory[31–33] for use in the IBO analysis at these geometries.

Let us begin by investigating the bonding between Au and the directly bound carbon atom $C^{Au/1}$ using the CD method. As described in the introduction, the Dewar-Chatt-Duncanson (DCD) components of the coordination bond are constructed

from σ-donation and π-backdonation. Through the CD method within the Natural Orbitals for Chemical Valence (NOCV) scheme, the π-backdonation component can be decomposed into two different contributions: one of them is parallel with respect to the plane described by $C(NHC)Au-C^{Au/1}-C^2-C^3$, whereas the other is perpendicular to it (they will be called parallel $\pi_\parallel$ and perpendicular $\pi_\perp$-backdonation, respectively).

The CD curves describing the diarylallenylidene to Au σ-donation are shown in Figure S1A in the Supporting Information. The most evident feature that can be pointed out is that the CD curves of all the complexes overlap almost perfectly. This indicates that the change of the R^1/R^2 substituents of the aromatic groups does not affect their σ-donation properties significantly. Since this high degree of overlap between the CD curves is also observed for parallel $\pi_\parallel$-backdonation, as shown in Figure S1B, we can conclude that this component is also unaffected by the variation of the substituents. In Table 1 the

Table 1. Computed Charge-Transfer CT values (in e^-) obtained from the CD-NOCV analysis for the series of complexes shown in Figure 1. The CT^{net} contribution is the net Charge Transfer obtained as sum of all the contributions. The CTσ don is the σ donation contribution, and CTπ-back⊥ and CTπ-back$^\parallel$ are the perpendicular and parallel π backdonation components, respectively.

Complex	CT^{net}	$CT^{\sigma-don}$	$CT^{\pi-back}_\perp$	$CT^{\pi-back}_\parallel$
a	0.18	0.34	−0.11	−0.03
b	0.19	0.34	−0.10	−0.03
c	0.20	0.34	−0.09	−0.03
d	0.21	0.34	−0.09	−0.03
e	0.22	0.34	−0.07	−0.03

calculated charge transfer (CT; net, σ-donation, $\pi_\parallel$- and $\pi_\perp$-backdonation values) are reported for all complexes.

As a general feature, we observe a large σ-donation towards the metal fragment (CT = 0.34 e^-, Table 1). In contrast, the parallel $\pi_\parallel$-backdonation is almost negligible – we find a CT value of only −0.03 e^- flowing from the metal fragment to the diarylallenylidene ligand (Table 1). However, we find positive values of the CD function which describe the parallel $\pi_\parallel$-backdonation at the $C^{Au/1}-C^2$ bond region. These demonstrate that the positively charged metal fragment exerts a polarization on the π-electron density, causing a charge depletion on C^2 and a charge accumulation on the $C^{Au/1}$ atom. This is also reflected in the isodensity surface shown in the inset in Figure S1B. We note here that the isosurfaces are increased significantly to clearly identify these small contributions.

In contrast to the σ-donation and the parallel $\pi_\parallel$-backdonation, the perpendicular $\pi_\perp$-backdonation component actually is affected by the change in substituents, as shown in Figure 2, the CD curves are clearly distinguishable, and reveal a well-defined trend. In the series of complexes **a** to **e**, the perpendicular $\pi_\perp$-backdonation bond component decreases simultaneously as the donor ability of the substituent increases. The CT values range from −0.11 e^- for complex **a** to −0.07 e^- for complex **e**. This variation is notable as the substitution pattern is changed seven atoms away from the gold fragment, suggesting efficient conjugation in the π perpendicular system.
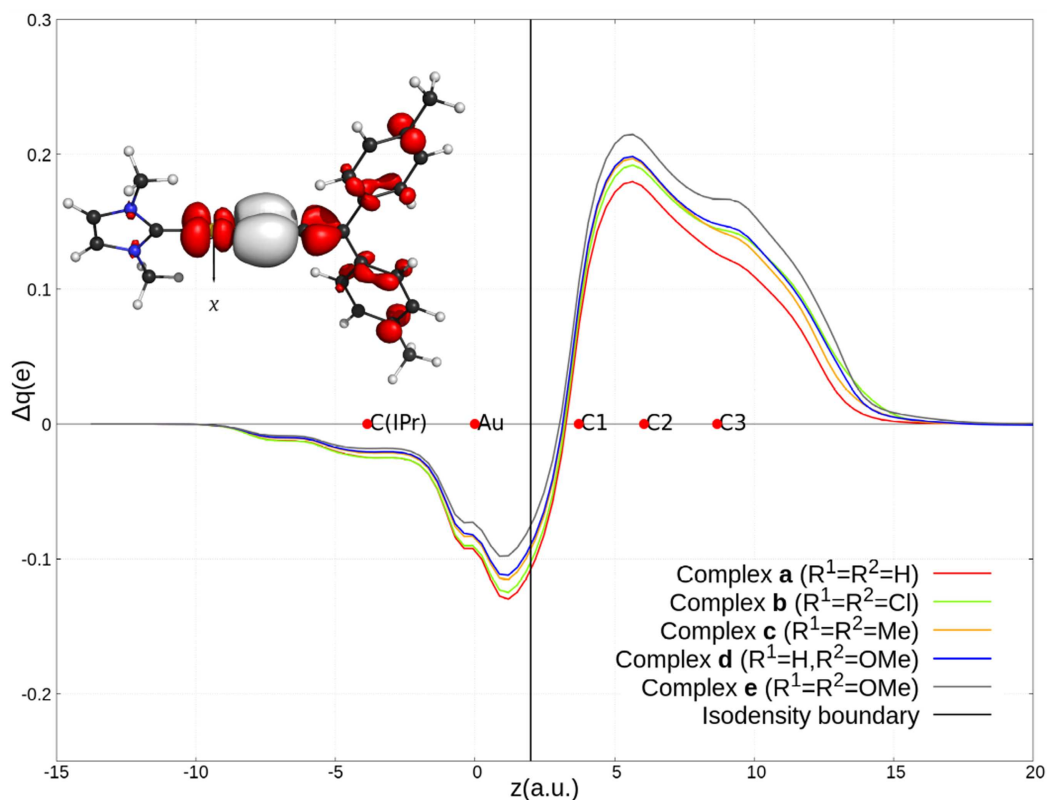
Figure 2. CD curves for the $\pi_\perp$-backdonation component of the Au-diarylallenylidene bond in the series of complexes in Figure 1. The z origin is placed at the Au atom for all complexes and red dots indicate the positions of Au, C atom of NHC ligand and C^1, C^2 and C^3 atoms in the diarylallenylidene ligand (averaged for all complexes). The inset shows the isodensity surface (± 0.0012 e a.u.$^{-3}$) of complex **c** for the perpendicular $\pi_\perp$-backdonation. Red surfaces represent charge depletion, whereas grey surfaces represent charge accumulation regions. Complex **c** is taken as example for the whole series of complexes.

This feature has been also found in non-conventional carbene complex chemistry, including gold carbenes, and it is known in the field as "remote stabilization".[37] In addition, this analysis shows that the perpendicular $\pi_\perp$-backdonation component ranges from 1/3 (complex **a**) to 1/5 (complex **e**) of the σ donation Au–$C^{Au/1}$ bond component values (Table 1). At this stage we therefore judge that, although a depiction of these complexes according to Lewis structures **I** and **III** in Figure 1 are the most appropriate, Lewis structure **II** cannot be completely neglected. The difference in donor ability of the substituents slightly modulates the relative weights of the two structures, with the Lewis structure **I** remaining dominant.

In order to probe how these changes in the Au–$C^{Au/1}$ bonding are reflected in the overall bonding in the allenylidene fragment, we carried out an IBO analysis (Figure 3).[15] In agreement with the CD analysis we find little π-backbonding. The partial charge distribution of the suitably oriented localized d-orbitals indicates minor overlap with $C^{Au/1}$ (0.074 and 0.026). The expected σ-donation to Au (green IBO) is also identified.

For the parallel π-system an IBO consistent with a well localized π-bond can be identified, with a partial charge distribution showing only minor polarization. In contrast, for the perpendicular π-system we not only need to account for the π-bond, but also for the conjugated aromatic system, which is directly influenced by variation of the substituents in

complexes **a**–**e**. Here the π-bond is polarized towards C^3 leading to a partial charge of 0.333 at this carbon atom. In addition, partial charges of 0.216 are identified from each aryl substituent on C^3. This simple picture is consistent with Lewis structure **III** in Figure 1, where a carbocation is stabilized through π-donation from these three IBOs. As a direct consequence a response of the appropriately oriented d-orbital, although small, is observed. Upon variation of the substituents on the aromatic groups, the perpendicular π-system directly responds. As the substituents on the aromatic groups become more donating, the overlap of the IBOs from the aromatic groups with C^3 increases and at the same time the donation of the π-bond decreases. Both effects are linearly correlated in magnitude, see Figure S2.

For Au carbene complexes[7] a similar trend was observed-namely, that upon an increase in donor ability due to the presence of electron donating substituents the IBO overlap with the Au-bound carbon increases. This trend could be correlated[7] with Hammett σ^+ values.[38] In the same way we can find a reasonable correlation of Hammett parameters with IBO overlap as described above, for complexes **a**–**e** (Figure S3). Notably, this correlation also applies to the perpendicular $\pi_\perp$-backdonation components.

As Hammett values are of experimental origin, we have established a direct connection between experiment and
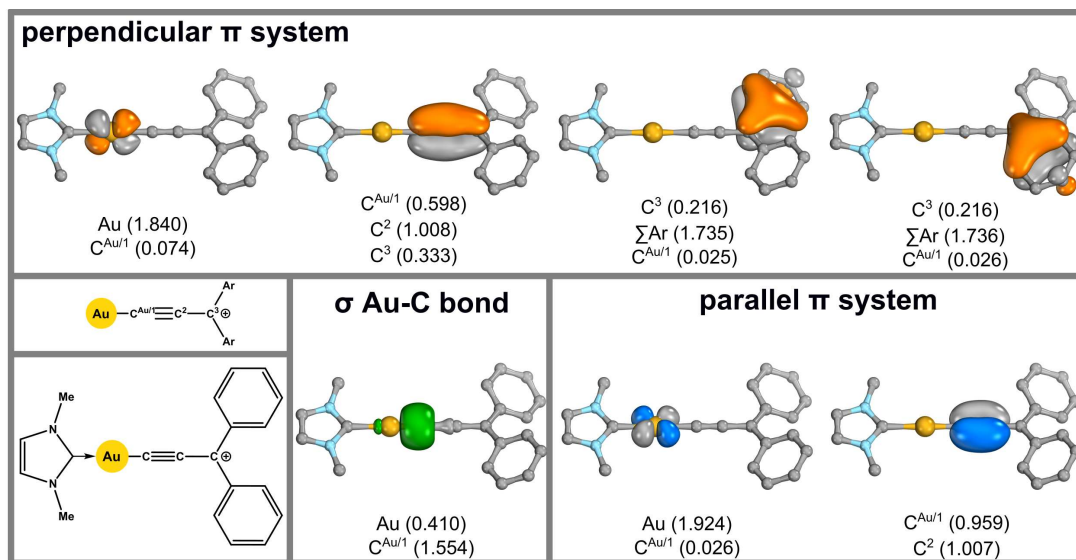
Figure 3. Intrinsic bond orbitals (IBOs) for complex **a**. Values in parenthesis are the partial charges for a given IBO assigned to the individual atoms. Structural depictions were made using IboView.[25a,39] Hydrogen atoms are removed for clarity.

theory. A direct comparison between experimental data specific to complexes **a**–**e** and theory can also be made based on the reported spectroscopic and reactivity data.

Based on both the CD and IBO analyses it can be expected that changes in the perpendicular π-system ought to be reflected in the spectroscopic features. The $C^{Au/1}$–C^2 stretching frequency, as determined by IR spectroscopy, provides a direct measure of bond strength and thus how much triple bond character is present. A plot of $\nu_{CAu/1-C2}$ versus the overlap of the sum of the aromatic substituents, as well as the relevant π-bond, with C^3 produces reasonable correlations (Figure 4A). In a very similar fashion one can correlate the CD which characterizes the Au–$C^{Au/1}$ interaction. Again, we find a linear correlation (Figure 4B) supporting that conjugation, and hence electronic communication, is facile in the perpendicular π-system. A correlation of the IBO partial charge overlap with the Au d-orbital relevant to the perpendicular π-backbonding equally correlates (Figure S4).

It is noteworthy that for complex **a** the stretching frequency $\nu_{CAu/1-C2}$ of 2051 cm^{-1}[4] is still reflective of significant alkyne character. Notably, the precursor featuring a OMe group bound to C^3 has a $\nu_{CAu/1-C2}$ stretching frequency of 2120 cm^{-1}, so the observed $\nu_{CAu/1-C2}$ in the complex shows a shift of merely 69 cm^{-1}.[4] Overall both this spectroscopic feature and our computational analyses identify Lewis structure **III** (shown in Figure 1) as the most suitable depiction of the bonding scenario in these complexes. We shall note here that in an early study Hashmi and co-workers already suggested that the alkyne character is largely retained in formal Au(I) allenylidene complexes possessing heteroatom stabilization.[3a] Thus, the stabilizing role attributed to heteroatoms in this context can be directly assigned to the aromatic groups present in the complexes studied here. In a similar way, the ^{13}C NMR shifts
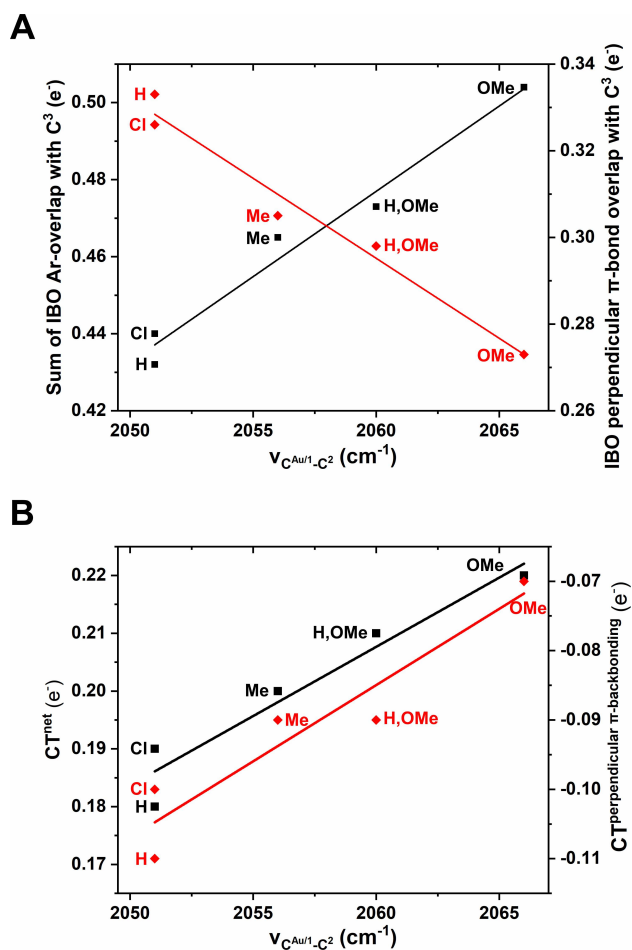
Figure 4. Correlation plots between the experimentally determined $\nu_{CAu/1-C2}$ stretching frequency[4] and A) the overlap with IBOs associated with the sum of the aromatic substituents [black squares] and the relevant π-bond with C^3 [red diamonds] and B) the total Charge Transfer (CT^{net}) [black squares] and the associated to the total perpendicular $\pi_\perp$-backdonation [red diamonds].

Table 2. Computed interaction energy ΔE_{int}, steric interaction energy ΔE^0, Pauli repulsion ΔE_{Pauli}, electrostatic interaction energy ΔE_{elect}, orbital interaction energy ΔE_{oi}, σ contribution (ΔE_{oi} (σ)), π out-of-plane (ΔE_{oi} ($\pi_\perp$)) and π in-plane (ΔE_{oi} ($\pi_\parallel$)) contributions to ΔE_{oi} and ΔG^+ for decomposition between the $[IPrAu]^+$ and $[C^3Ar_2]$ fragments for the series of complexes shown in Figure 1. All energy values are given in kcal mol^{-1}.

Complex	ΔE_{int}	ΔE^0	ΔE_{Pauli}	ΔE_{elect}	ΔE_{oi}	ΔE_{oi} (σ)	ΔE_{oi} ($\pi_\perp$)	ΔE_{oi} ($\pi_\parallel$)	$\Delta G^{+[4]}$
a	−97.01	−11.64	183.72	−195.36	−85.37	−44.13	−18.61	−10.14	15.4
b	−96.03	−10.15	183.14	−193.29	−85.88	−44.11	−18.97	−10.16	15.9
c	−100.18	−14.44	184.57	−199.01	−85.73	−44.47	−18.30	−9.96	20.4
d	−101.14	−15.51	184.37	−199.88	−85.62	−44.51	−18.22	−9.92	21.1
e	−104.32	−18.41	184.96	−203.36	−85.92	−44.83	−17.88	−9.73	22.9

show linear correlations (Figure S5) lending further support to the interpretation outlined above.

In their study, Kim and Widenhoefer also determined rates for decomposition of complexes **a**–**e**.[4] Using energy decomposition analysis (EDA) we investigated if there is a correlation between the Au–C$^{Au/1}$ bonding and ΔG^+ for decomposition. EDA results are shown in Table 2.

Interestingly, we find that the barrier heights for decomposition show a linear correlation with the interaction energy (ΔE_{int}) (Figure 5). This immediately raises the question of which
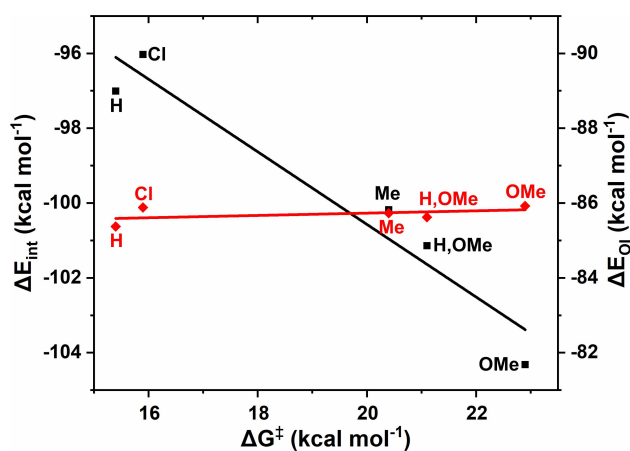
Figure 5. Correlation plot between experimentally determined barriers for decomposition (ΔG^+) and calculated interaction energy (ΔE_{int}) and the orbital interaction energy (ΔE_{oi}).

component of the Au–C$^{Au/1}$ interaction builds the foundation for this correlation. From the bonding analysis one might be tempted to attribute the increased stability to the variation of π-backbonding. The σ, out-of-plane and in-plane π energy contributions in Table 2 are consistent with the corresponding CT values in Table 1. The largest contribution to ΔE_{oi} is due to the σ-donation, coherently with the large σ-donation CT value in the Au–C bonding, with the perpendicular $\pi_\perp$-backdonation energy contribution amounting to about 21% of the total ΔE_{oi} which in turn accounts for 82–88% of the total interaction energy ΔE_{oi} but for only 42–44% of the electrostatic interaction ΔE_{elect} between the gold fragment and the diarylallenylidene ligand (Table 2). The parallel $\pi_\parallel$-backdonation energy contribution is much smaller than the perpendicular $\pi_\perp$-backdonation one, in agreement with the smallest parallel $\pi_\parallel$-backdonation

Au–C bond component. The variation trend of ΔE_{oi} and its σ and π contributions along the series of complexes (Table 2) also matches that of the CT^{net} and its σ and π components (Table 1). Note that the σ and π energy contributions from EDA also include polarization effects. Analogously, using the CDA and EDA methods for the study of the transition metal carbene and gold carbene bond, Frenking and co-workers[40] found that, although the metal-ligand π interaction is certainly not "negligible" compared to the σ interaction, it constitutes less than 20% of the total orbital interaction energy, although the latter accounts for only 22–25% of the total interaction energy between gold and the carbene ligand in these systems. A comparative study of N- and P-heterocyclic carbenes and their gold complexes by Jacobsen[41] demonstrated that PHCs are better π-acceptor than NHCs, increasing the π percentage contribution to the total orbital interaction from $\leq 20\%$ up to 45%.

It is worth noting that, in the Au(I) diarylallenylidene complexes studied here, however, the perpendicular $\pi_\perp$-back-donation ΔE_{oi} ($\pi_\perp$) energy contribution varies only slightly along the series (by about 1.1 kcal mol^{-1}). Analogously, the orbital interaction energy (ΔE_{oi}) merely varies by <1 kcal mol^{-1} for complexes **a**–**e** as can be seen from Figure 5, and it turns out to be the quasi-classical electrostatic interaction term (ΔE_{elst}) that corresponds to these changes. This electrostatic interaction can be ascribed to a different charge redistribution on the C^1 atom of the organic fragment, depending on the substituents via electronic π-delocalization, consistently with the Voronoi Deformation Density atomic charge[42] variation on C^1 ranging from −0.155 to −0.182 e$^-$ from complexes **a** to **e**, where the Au–C^1 distance value remains almost constant along the series (1.960–1.965 Å) (see Table S7).

3. Conclusions

In summary, we have demonstrated that Au(I) allenylidene complexes are governed by large σ-donation and small π-backdonation of the Au–C bonding as evidenced both by CD and IBO approaches. Nevertheless, the π-backbonding can be modulated by the donor ability of the aryl substituents. The IBO approach further reveals the importance of the π-donation of the aromatic groups which is stabilizing the carbocation, and which can be tuned by variation of the substituents. The computed trends are in excellent agreement with the previously reported spectroscopic features and the observed stability

of the complexes. Therefore, the aromatic groups take the role of stabilizing these complexes through π-donation, which is commonly performed by heteroatoms (cf. Figure 1). Notably, this effect has also been exploited in the preparation of Au carbene complexes.[6,9–10] With respect to the most appropriate Lewis structure description, we conclude that depiction **III** shown in Figure 1 is most appropriate, especially as it indicates the contribution from the π-donation of the aromatic rings. Nevertheless, depending on the substituent, some contribution from Lewis structure **II** may not be totally neglected. In order to render the electronic structure of the complexes discussed here and related structures more allenylidene-like, a significant reduction in the π-donation from the aromatic substituents, and by extension heteroatom stabilization, is required. Alternatively, one could also envision that the coordination environment around Au might be modulated to increase the π-backbonding and thus increase the contribution of Lewis structure **II**, as has been realized with carborane based ligands for carbene complexes before.[10]

Acknowledgements

Conflict of Interest

The authors declare no conflict of interest.

Keywords: allenylidene · computational chemistry · electronic structure · Gold · Lewis structures.

[1] C. J. V. Halliday, J. M. Lynam, *Dalton Trans.* **2016**, *45*, 12611–12626.
[2] a) A. Hoffmann-Röder, N. Krause, *Org. Biomol. Chem.* **2005**, *3*, 387–391; b) A. S. K. Hashmi, G. J. Hutchings, *Angew. Chem. Int. Ed.* **2006**, *45*, 7896–7936; c) E. Jiménez-Núñez, A. M. Echavarren, *Chem. Commun.* **2007**, 333–346; d) A. S. K. Hashmi, *Chem. Rev.* **2007**, *107*, 3180–3211; e) Z. Li, C. Brouwer, C. He, *Chem. Rev.* **2008**, *108*, 3239–3265.
[3] a) M. M. Hansmann, F. Rominger, A. S. K. Hashmi, *Chem. Sci.* **2013**, *4*, 1552–1559; b) X.-S. Xiao, W.-L. Kwong, X. Guan, C. Yang, W. Lu, C.-M. Che, *Chem. Eur. J.* **2013**, *19*, 9457–9462; c) L. Jin, M. Melaimi, A. Kostenko, M. Karni, Y. Apeloig, C. E. Moore, A. L. Rheingold, G. Bertrand, *Chem. Sci.* **2016**, *7*, 150–154; d) X.-S. Xiao, C. Zou, X. Guan, C. Yang, W. Lu, C.-M. Che, *Chem. Commun.* **2016**, *52*, 4983–4986.
[4] N. Kim, R. A. Widenhoefer, *Angew. Chem. Int. Ed.* **2018**, *57*, 4722–4726.
[5] R. Peloso, E. Carmona, *Coord. Chem. Rev.* **2018**, *355*, 116–132.
[6] G. Seidel, A. Fürstner, *Angew. Chem. Int. Ed.* **2014**, *53*, 4807–4811.
[7] L. Nunes dos Santos Comprido, J. E. M. N. Klein, G. Knizia, J. Kästner, A. S. K. Hashmi, *Angew. Chem. Int. Ed.* **2015**, *54*, 10336–10340.
[8] R. J. Harris, R. A. Widenhoefer, *Angew. Chem. Int. Ed.* **2014**, *53*, 9369–9371.
[9] M. W. Hussong, F. Rominger, P. Krämer, B. F. Straub, *Angew. Chem. Int. Ed.* **2014**, *53*, 9372–9375.
[10] M. Joost, L. Estévez, S. Mallet-Ladeira, K. Miqueu, A. Amgoune, D. Bourissou, *Angew. Chem. Int. Ed.* **2014**, *53*, 14512–14516.
[11] a) A. S. K. Hashmi, *Angew. Chem. Int. Ed.* **2008**, *47*, 6754–6756; b) D. Benitez, N. D. Shapiro, E. Tkatchouk, Y. Wang, W. A. Goddard III, F. D. Toste, *Nat. Chem.* **2009**, *1*, 482; c) A. M. Echavarren, *Nat. Chem.* **2009**, *1*, 431; d) Y. Wang, M. E. Muratore, A. M. Echavarren, *Chem. Eur. J.* **2015**, *21*, 7332–7339; e) R. J. Harris, R. A. Widenhoefer, *Chem. Soc. Rev.* **2016**, *45*, 4533–4551; f) D. Munz, *Organometallics* **2018**, *37*, 275–289.
[12] a) L. Belpassi, I. Infante, F. Tarantelli, L. Visscher, *J. Am. Chem. Soc.* **2008**, *130*, 1048–1060; b) N. Salvi, L. Belpassi, F. Tarantelli, *Chem. Eur. J.* **2010**, *16*, 7231–7240; c) G. Bistoni, S. Rampino, F. Tarantelli, L. Belpassi, *J. Chem. Phys.* **2015**, *142*, 084112; d) G. Ciancaleoni, L. Biasiolo, G. Bistoni, A. Macchioni, F. Tarantelli, D. Zuccaccia, L. Belpassi, *Chem. Eur. J.* **2015**, *21*, 2467–2473; e) G. Bistoni, L. Belpassi, F. Tarantelli, *Angew. Chem. Int. Ed.* **2013**, *52*, 11599–11602.
[13] a) M. J. S. Dewar, *Bull. Soc. Chim. Fr.* **1951**, *18*, C71–C79; b) J. Chatt, L. A. Duncanson, *J. Chem. Soc.* **1953**, 2939–2947.
[14] L. Nunes dos Santos Comprido, J. E. M. N. Klein, G. Knizia, J. Kästner, A. S. K. Hashmi, *Chem. Eur. J.* **2016**, *22*, 2892–2895.
[15] G. Knizia, *J. Chem. Theory Comput.* **2013**, *9*, 4834–4843.
[16] a) M. Mitoraj, A. Michalak, *J. Mol. Model.* **2007**, *13*, 347–355; b) A. Michalak, M. Mitoraj, T. Ziegler, *J. Phys. Chem. A* **2008**, *112*, 1933–1939.
[17] a) R. F. Nalewajski, J. Mrozek, *Int. J. Quantum Chem.* **1994**, *51*, 187–200; b) R. F. Nalewajski, J. Mrozek, A. Michalak, *Int. J. Quantum Chem.* **1997**, *61*, 589–601; c) A. Michalak, R. L. DeKock, T. Ziegler, *J. Phys. Chem. A* **2008**, *112*, 7256–7263.
[18] M. P. Mitoraj, A. Michalak, T. Ziegler, *J. Chem. Theory Comput.* **2009**, *5*, 962–975.
[19] L. Biasiolo, L. Belpassi, C. A. Gaggioli, A. Macchioni, F. Tarantelli, G. Ciancaleoni, D. Zuccaccia, *Organometallics* **2016**, *35*, 595–604.
[20] C. A. Gaggioli, G. Bistoni, G. Ciancaleoni, F. Tarantelli, L. Belpassi, P. Belanzoni, *Chem. Eur. J.* **2017**, *23*, 7558–7569.
[21] C. A. Gaggioli, L. Belpassi, F. Tarantelli, J. N. Harvey, P. Belanzoni, *Dalton Trans.* **2017**, *46*, 11679–11690.
[22] D. Sorbelli, L. Belpassi, F. Tarantelli, P. Belanzoni, *Inorg. Chem.* **2018**, *57*, 6161–6175.
[23] a) K. Morokuma, *J. Chem. Phys.* **1971**, *55*, 1236–1244; b) T. Ziegler, A. Rauk, *Theor. Chim. Acta* **1977**, *46*, 1–10; c) M. v. Hopffgarten, G. Frenking, *WIREs Comput. Mol. Sci.* **2012**, *2*, 43–62.
[24] J. Pipek, P. G. Mezey, *J. Chem. Phys.* **1989**, *90*, 4916–4926.
[25] a) G. Knizia, J. E. M. N. Klein, *Angew. Chem. Int. Ed.* **2015**, *54*, 5518–5522; b) L. Nunes Dos Santos Comprido, J. E. M. N. Klein, G. Knizia, J. Kästner, A. S. K. Hashmi, *Chem. Eur. J.* **2017**, *23*, 10901–10905; c) J. E. M. N. Klein, G. Knizia, L. Nunes dos Santos Comprido, J. Kästner, A. S. K. Hashmi, *Chem. Eur. J.* **2017**, *23*, 16097–16103; d) J. E. M. N. Klein, G. Knizia, *Angew. Chem. Int. Ed.* **2018**, *57*, 11913–11917.
[26] a) C. Fonseca Guerra, J. G. Snijders, G. te Velde, E. J. Baerends, *Theor. Chem. Acc.* **1998**, *99*, 391–403; b) G. te Velde, F. M. Bickelhaupt, E. J. Baerends, C. Fonseca Guerra, S. J. A. van Gisbergen, J. G. Snijders, T. Ziegler, *J. Comput. Chem.* **2001**, *22*, 931–967.
[27] a) J. P. Perdew, *Phys. Rev. B* **1986**, *33*, 8822–8824; b) A. D. Becke, *Phys. Rev. A* **1988**, *38*, 3098–3100; c) J. P. Perdew, *Phys. Rev. B* **1986**, *34*, 7406–7406.
[28] E. Van Lenthe, E. J. Baerends, *J. Comput. Chem.* **2003**, *24*, 1142–1156.
[29] a) E. Van Lenthe, E. J. Baerends, J. G. Snijders, *J. Chem. Phys.* **1993**, *99*, 4597–4610; b) E. Van Lenthe, E. J. Baerends, J. G. Snijders, *J. Chem. Phys.* **1994**, *101*, 9783–9792; c) E. Van Lenthe, A. Ehlers, E. J. Baerends, *J. Chem. Phys.* **1999**, *110*, 8943–8953.
[30] a) F. Furche, R. Ahlrichs, C. Hättig, W. Klopper, M. Sierka, F. Weigend, *WIREs Comput. Mol. Sci.* **2014**, *4*, 91–100; b) R. Ahlrichs, M. Bär, M. Häser, H. Horn, C. Kölmel, *Chem. Phys. Lett.* **1989**, *162*, 165–169; c) TURBOMOLE V7.0.2 2015, a development of University of Karlsruhe and Forschungszentrum Karlsruhe GmbH, 1989–2007, TURBOMOLE GmbH, since 2007; available from http://www.turbomole.com.
[31] J. Tao, J. P. Perdew, V. N. Staroverov, G. E. Scuseria, *Phys. Rev. Lett.* **2003**, *91*, 146401.
[32] a) S. Grimme, J. Antony, S. Ehrlich, H. Krieg, *J. Chem. Phys.* **2010**, *132*, 154104; b) S. Grimme, S. Ehrlich, L. Goerigk, *J. Comput. Chem.* **2011**, *32*, 1456–1465.
[33] F. Weigend, R. Ahlrichs, *Phys. Chem. Chem. Phys.* **2005**, *7*, 3297–3305.
[34] D. Andrae, U. Häußermann, M. Dolg, H. Stoll, H. Preuß, *Theor. Chim. Acta* **1990**, *77*, 123–141.
[35] M. Sierka, A. Hogekamp, R. Ahlrichs, *J. Chem. Phys.* **2003**, *118*, 9136–9148.
[36] F. Weigend, *Phys. Chem. Chem. Phys.* **2006**, *8*, 1057–1065.

[37] a) R. Lalrempuia, N. D. McDaniel, H. Müller-Bunz, S. Bernhard, M. Albrecht, *Angew. Chem. Int. Ed.* **2010**, *49*, 9765–9768; b) H. G. Raubenheimer, S. Cronje, *Chem. Soc. Rev.* **2008**, *37*, 1998–2011.

[38] H. C. Brown, Y. Okamoto, *J. Am. Chem. Soc.* **1958**, *80*, 4979–4987.

[39] G. Knizia, *http://www.iboview.org/*.

[40] a) G. Frenking, M. Solà, S. F. Vyboishchikov, *J. Organomet. Chem.* **2005**, *690*, 6178–6204; b) D. Nemcsok, K. Wichmann, G. Frenking, *Organometallics* **2004**, *23*, 3640–3646.

[41] H. Jacobsen, *J. Organomet. Chem.* **2005**, *690*, 6068–6078.

[42] C. Fonseca Guerra, J.-W. Handgraaf, E. J. Baerends, F. M. Bickelhaupt, *J. Comput. Chem.* **2004**, *25*, 189–210.